nature medicine

A recombinant *Mycobacterium smegmatis* induces potent bactericidal immunity against *Mycobacterium tuberculosis*

Kari A Sweeney[1,2], Dee N Dao[1,2,6], Michael F Goldberg[2,6], Tsungda Hsu[1,2], Manjunatha M Venkataswamy[2], Marcela Henao-Tamayo[3], Diane Ordway[3], Rani S Sellers[4], Paras Jain[1,2], Bing Chen[1,2], Mei Chen[1,2], John Kim[1,2], Regy Lukose[1,2], John Chan[2,5], Ian M Orme[3], Steven A Porcelli[2,5] & William R Jacobs Jr[1,2,5]

We report the involvement of an evolutionarily conserved set of mycobacterial genes, the *esx-3* region, in evasion of bacterial killing by innate immunity. Whereas high-dose intravenous infections of mice with the rapidly growing mycobacterial species *Mycobacterium smegmatis* bearing an intact *esx-3* locus were rapidly lethal, infection with an *M. smegmatis* Δ*esx-3* mutant (here designated as the IKE strain) was controlled and cleared by a MyD88-dependent bactericidal immune response. Introduction of the orthologous *Mycobacterium tuberculosis esx-3* genes into the IKE strain resulted in a strain, designated IKEPLUS, that remained susceptible to innate immune killing and was highly attenuated in mice but had a marked ability to stimulate bactericidal immunity against challenge with virulent *M. tuberculosis*. Analysis of these adaptive immune responses indicated that the highly protective bactericidal immunity elicited by IKEPLUS was dependent on CD4$^+$ memory T cells and involved a distinct shift in the pattern of cytokine responses by CD4$^+$ cells. Our results establish a role for the *esx-3* locus in promoting mycobacterial virulence and also identify the IKE strain as a potentially powerful candidate vaccine vector for eliciting protective immunity to *M. tuberculosis*.

Tuberculosis is a leading cause of global mortality due to infectious disease, and it is a worsening problem owing to HIV co-infection and the emergence of extremely drug-resistant strains of *M. tuberculosis* (Mtb)[1,2]. The only currently used vaccine, the attenuated *Mycobacterium bovis* strain bacille Calmette-Guérin (BCG), has been inconsistent in providing protection from disease, with low or unmeasurable efficacy in many of those regions with the most cases[1,3,4]. Moreover, BCG can cause severe, disseminated infection in HIV-positive infants, further restricting its use in areas with high prevalence of tuberculosis[5]. Animal models of tuberculosis also demonstrate that BCG vaccination generates at best partial immunity against Mtb that does not give complete control or clearance of infection[6]. Thus, new tuberculosis vaccines that are safer and more efficacious than BCG are clearly needed[7–9].

Generation of more effective vaccines requires a better understanding of the mechanisms by which Mtb evades innate and adaptive immune responses[6,10–14]. Some of these mechanisms are known to involve the export of various effector molecules by specialized bacterial secretion systems. For example, the well-studied mycobacterial type VII secretion system known as ESX-1 has been shown to be involved in a range of effects that promote mycobacterial virulence through secretion of the protein ESAT-6 and other effector proteins[15–25]. Notably, the Mtb genome encodes four other potential secretion systems that are paralogs of ESX-1 (designated ESX-2 through ESX-5), but their functions are mostly unknown. Although all mycobacterial species studied to date have between two and five of the *esx* loci, only the *esx-3* genes (comprising the genes *Rv0282* to *Rv0292* in Mtb and *Ms0615* to *Ms0626* in *M. smegmatis* (Msmeg); **Supplementary Fig. 1**) are conserved in all cases[26,27]. This suggests a unique and crucial function for ESX-3. Expression of *esx-3* genes is regulated by iron and zinc and is increased in the lungs of mice during persistent infection with Mtb[28–31], suggesting it may have a key role in virulence. In addition, an intact *esx-3* locus has been shown to be essential for the growth of Mtb in culture[32–34].

Because inactivation of *esx-3* is incompatible with viability in Mtb, in the current study we have used Msmeg, a mycobacterium that is able to grow without an intact *esx-3* locus, to study the influence of this locus on the innate and adaptive immune systems of the host. We observed loss of the ability to evade bactericidal host innate immunity for the Msmeg strain with deletion of *esx-3*, which we therefore designated by the acronym IKE to signify 'immune killing evasion', which is lost in this strain. Although insertion of the *esx-3* genes of Mtb into IKE did not reverse the susceptibility of the bacteria to innate immune killing, it did produce a recombinant strain, designated IKEPLUS, that induced a previously unobserved level of bactericidal immunity against Mtb. This new immunization strategy suggests an approach to tuberculosis vaccine development that can potentially induce sterilizing immunity and also reveals a previously undocumented capacity for the mammalian immune system to eliminate virulent mycobacteria from infected tissues.

[1]Howard Hughes Medical Institute, Albert Einstein College of Medicine, Bronx, New York, USA. [2]Department of Microbiology and Immunology, Albert Einstein College of Medicine, Bronx, New York, USA. [3]Department of Microbiology, Immunology and Pathology, Colorado State University, Fort Collins, Colorado, USA. [4]Department of Pathology, Albert Einstein College of Medicine, Bronx, New York, USA. [5]Department of Medicine, Albert Einstein College of Medicine, Bronx, New York, USA. [6]These authors contributed equally to this work. Correspondence should be addressed to W.R.J. (jacobsw@hhmi.org).

Received 18 April; accepted 14 June; published online 4 September 2011; doi:10.1038/nm.2420

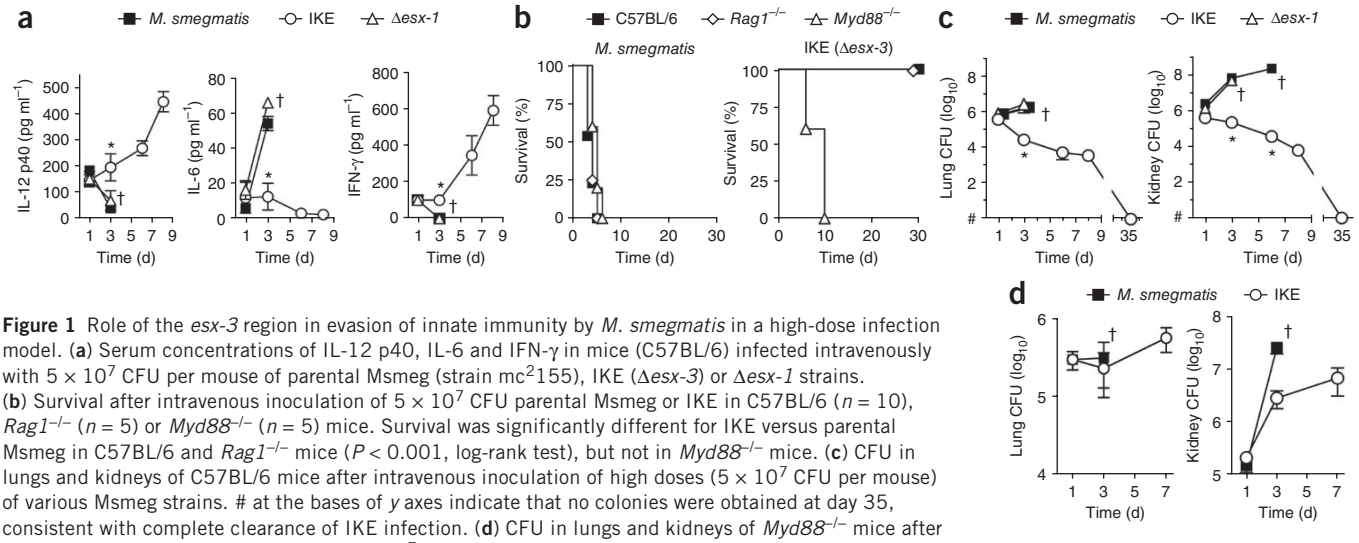

Figure 1 Role of the *esx-3* region in evasion of innate immunity by *M. smegmatis* in a high-dose infection model. (**a**) Serum concentrations of IL-12 p40, IL-6 and IFN-γ in mice (C57BL/6) infected intravenously with 5×10^7 CFU per mouse of parental Msmeg (strain mc^2155), IKE (Δ*esx-3*) or Δ*esx-1* strains. (**b**) Survival after intravenous inoculation of 5×10^7 CFU parental Msmeg or IKE in C57BL/6 ($n = 10$), *Rag1*$^{-/-}$ ($n = 5$) or *Myd88*$^{-/-}$ ($n = 5$) mice. Survival was significantly different for IKE versus parental Msmeg in C57BL/6 and *Rag1*$^{-/-}$ mice ($P < 0.001$, log-rank test), but not in *Myd88*$^{-/-}$ mice. (**c**) CFU in lungs and kidneys of C57BL/6 mice after intravenous inoculation of high doses (5×10^7 CFU per mouse) of various Msmeg strains. # at the bases of *y* axes indicate that no colonies were obtained at day 35, consistent with complete clearance of IKE infection. (**d**) CFU in lungs and kidneys of *Myd88*$^{-/-}$ mice after intravenous inoculation of high doses (5×10^7 CFU per mouse) of various Msmeg strains. For **a**, **c** and **d**, data are mean ± s.e.m. of three mice per group. † indicates death or killing owing to extreme morbidity of all mice in a group; $^*P < 0.01$ (analysis of variance (ANOVA)). Data for all panels are representative of six independent experiments.

RESULTS

Role of *esx-3* in evasion of innate immunity

A robust T helper type 1 (T_H1) cell response has a key role in protective immunity to many intracellular pathogens and may be crucial for effective immunity to Mtb[35]. To assess mechanisms by which mycobacteria may interfere with development of T_H1 cell responses, we analyzed the cytokines induced *in vivo* in mice after infection with Msmeg mutants with deletions of the *esx-1* and *esx-3* loci (**Supplementary Fig. 2**). We constructed these mutants in Msmeg because of previous work indicating that *esx-3* cannot be deleted in Mtb, probably because of its essential role in iron acquisition[32,34]. This is not the case for Msmeg because of the presence of a second siderophore system (exochelin) in that species. As expected, a Δ*esx-3* Msmeg strain (IKE) was readily isolated and grew normally in iron-replete or iron-deficient medium (**Supplementary Fig. 3a**). We infected mice intravenously with high doses of either unmodified parental, Δ*esx-1* or IKE strains of Msmeg and measured serum cytokine concentrations. Whereas parental and Δ*esx-1* Msmeg induced low or undetectable levels of the interleukin-12 (IL-12) subunit p40 and interferon-γ (IFN-γ), infection with IKE elicited robust secretion of these cytokines. In contrast, IL-6 was strongly induced by parental and Δ*esx-1* Msmeg but was barely detectable in IKE-infected mice (**Fig. 1a**).

Although Msmeg is a saprophytic organism and generally not considered pathogenic, we found that a high intravenous dose ($\geq 1 \times 10^7$ colony-forming units (CFU)) of parental or Δ*esx-1* Msmeg was uniformly fatal in C57BL/6 mice within 7 d (**Fig. 1b** and data not shown). Administration of the same number of heat-killed or ultraviolet-irradiated bacteria did not result in death (**Supplementary Fig. 3b**). In clear contrast, all C57BL/6 mice infected with the IKE mutant survived and cleared their infections without apparent sequelae (**Fig. 1b**). The attenuation of Msmeg IKE was further underscored by its inability to kill recombination-activating gene-1–null mice (*Rag1*$^{-/-}$), which lack T and B cells (**Fig. 1b**), suggesting control of infection by an innate immune response. To explore this possibility, we infected a panel of mouse strains deficient in various innate immune response genes (**Supplementary Table 1**). Among these, only mice lacking the adaptor protein MyD88 were unable to clear the Msmeg IKE infection and died with kinetics similar to those observed in mice infected with parental Msmeg (**Fig. 1b** and **Supplementary Table 1**).

Whereas histological analysis of C57BL/6 mice infected with high-dose (5×10^7 CFU) intravenous parental Msmeg showed substantial pathology in the brain, spleen and liver and particularly in the kidney, mice infected with IKE showed no notable pathology in these tissues (data not shown). To further study the attenuation of IKE, we determined tissue bacterial burdens after high-dose intravenous infection of C57BL/6, *Rag1*$^{-/-}$ and *Myd88*$^{-/-}$ mice. For C57BL/6 and *Rag1*$^{-/-}$ mice, there was rapid clearance of IKE from the lungs and kidneys as early as day 3 after infection, with complete clearance by day 35, whereas the parental and Δ*esx-1* Msmeg strains showed increasing tissue bacterial burdens during the 3–6 d before death of the mice (**Fig. 1c**). In contrast, in *Myd88*$^{-/-}$ mice there was expansion of IKE bacilli after inoculation (**Fig. 1d**). These findings indicated that a previously unappreciated function of the genes in the *esx-3* region is to mediate evasion of a MyD88-dependent innate immune response that normally triggers bactericidal effects and host resistance to Msmeg infection.

We performed a genetic complementation analysis by introducing an integrating cosmid encoding all genes of Msmeg *esx-3* (*Ms0609–Ms0637*) into IKE to generate a strain that showed a partial restoration of virulence, as assessed by tissue bacterial burden (**Supplementary Fig. 4a**). The failure to completely complement the mutation may have been due to aberrant regulation of the introduced *esx-3* genes because of integration into a non-native location on the chromosome. We also infected mice with a strain of Msmeg that had a deletion in only a single *esx-3* gene (*Ms0615*), which showed alterations in cytokine patterns and an attenuation of virulence that were similar to those of IKE (**Supplementary Fig. 4b,c**). Although we have not determined whether the deletion of *Ms0615* has effects on other *esx-3* genes, it is noteworthy that complementation of this deletion with a plasmid encoding the entire Msmeg *esx-3* region (*Ms0600–Ms0624*) fully reversed the phenotype of the mutant in *Rag1*$^{-/-}$ mice (**Supplementary Fig. 4b–d**).

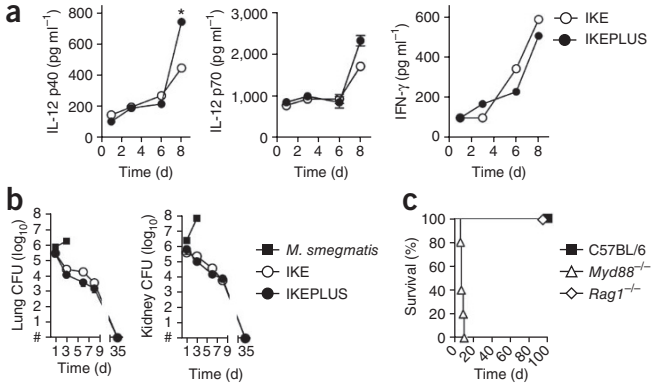

Figure 2 Characterization of innate immune responses against the Msmeg IKEPLUS strain. (**a**) Serum concentrations of IL-12 p40, IL-12p70 and IFN-γ in C57BL/6 mice infected with IKE or IKEPLUS (*$P < 0.01$, ANOVA with Bonferroni post-test). (**b**) Growth of bacteria (CFU) in the lungs (left) and kidneys (right) of *Rag1*$^{-/-}$ mice after intravenous inoculation of Msmeg parental, IKE or IKEPLUS strains. Differences in CFU were statistically significant ($P < 0.001$, two-way ANOVA) for Msmeg versus either IKE or IKEPLUS at day 3. # at the bases of *y* axes indicate that no colonies were obtained at day 35, consistent with complete clearance of IKE and IKEPLUS. (**c**) Average time to death of mice after intravenous inoculation of IKEPLUS in C57BL/6 ($n = 10$), *Rag1*$^{-/-}$ ($n = 5$) and *Myd88*$^{-/-}$ ($n = 5$) mice. Survival of wild-type C57BL/6 and *Rag1*$^{-/-}$ strains was significantly different than that of *Myd88*$^{-/-}$ mice ($P < 0.05$, log-rank test). All inoculations were done at a high intravenous dose (5×10^7 CFU per mouse). Data from **a** and **b** are mean ± s.e.m. of three mice per group. Data for all panels are representative of four independent experiments.

Generation and characterization of IKEPLUS

In contrast to our results with Msmeg and similar to previous studies, we were unable to isolate *esx-3* deletion mutants of Mtb[32,34]. As an alternative approach to study the function of Mtb *esx-3*, we assessed whether the orthologous Mtb genes could complement the Msmeg Δ*esx-3* phenotype. Thus, we introduced the orthologous locus of Mtb (*Rv0282–Rv0292*) into the IKE strain by transformation with cosmid pYUB1336 containing Mtb genes *Rv0278–Rv0303* (**Supplementary Table 2**), generating IKEPLUS. Despite the high homology of these regions between Mtb and Msmeg (minimum of 44% and up to 85% homology at the protein level for the 11 ORFs), analysis of the immunological properties and virulence of IKEPLUS indicated that the Mtb *esx-3* genes were unable to complement the phenotype associated with deletion of the Msmeg *esx-3* locus. Thus, measurements of serum cytokine concentrations showed that IKEPLUS induced robust IL-12 p40, p70 and IFN-γ responses similar to those observed with the IKE mutant (**Fig. 2a**). In spite of the stable integration of the Mtb *esx-3* genes into the IKE genome (**Supplementary Fig. 5**), the IKEPLUS strain was rapidly cleared from tissues (**Fig. 2b**) and was unable to kill either immunocompetent or *Rag1*$^{-/-}$ mice but was lethal in MyD88-deficient mice (**Fig. 2c**).

Ability of IKEPLUS to elicit bactericidal immunity against Mtb

The results presented above revealed properties of IKE and IKEPLUS that are desirable for antituberculosis vaccines. These mutants were highly attenuated for virulence in mice, thus fulfilling initial safety requirements, and they rapidly induced a cytokine milieu that was favorable to priming of T_H1 responses (**Fig. 2a**). Furthermore, in the case of IKEPLUS, this recombinant Msmeg contained a cosmid (pYUB1336, **Supplementary Table 2**; also see **Supplementary Table 3**) encoding 26 open reading frames of Mtb that had the potential to serve as specific antigens for eliciting adaptive immune responses that could be recalled by subsequent Mtb infection. To examine its potential as an antituberculosis vaccine, we used IKEPLUS to immunize mice (5×10^7 CFU intravenously), which we then challenged 8 weeks later with a high intravenous dose (1×10^7 CFU) of Mtb (virulent strain H37Rv). We immunized control groups either with saline or subcutaneously with BCG (1×10^7 CFU per mouse). The average time to death after Mtb challenge was 54 d for sham-vaccinated mice and 65 d for BCG-immunized mice, whereas the IKEPLUS-immunized mice had a mean survival time of 135 d (**Fig. 3a**).

Consistent with the extension of survival observed in a subset of IKEPLUS-immunized mice, we found in three separate experiments that intravenous immunization of mice with IKEPLUS led to marked reductions in tissue bacterial burdens in mice surviving to later time

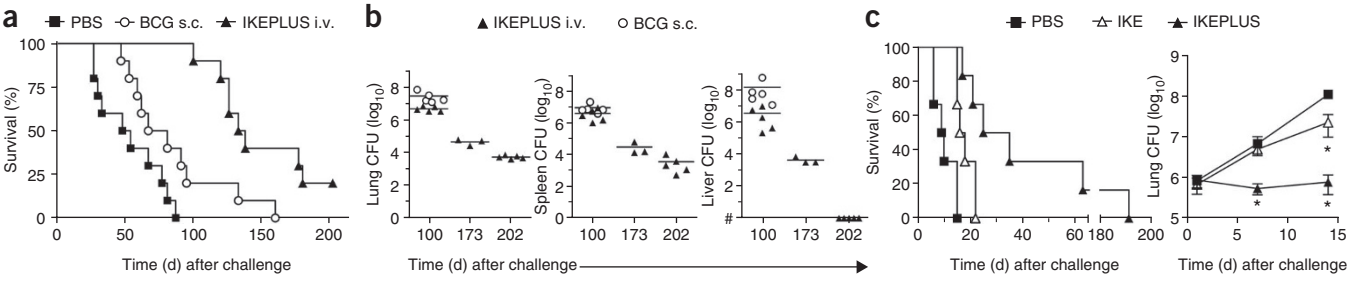

Figure 3 Bactericidal immunity against Mtb in mice vaccinated with IKEPLUS. (**a**) Survival of C57BL/6 mice that were sham immunized (intravenous (i.v.) PBS injection; $n = 21$) or immunized by intravenous infection with IKEPLUS (5×10^7 CFU per mouse; $n = 20$) or by subcutaneous (s.c.) infection with BCG (1×10^7 CFU per mouse; $n = 18$) and subsequently challenged 8 weeks later with a high intravenous dose (1×10^7 CFU per mouse) of Mtb H37Rv. Differences in survival were significant for PBS versus BCG ($P = 0.0389$, log-rank test), PBS versus IKEPLUS ($P < 0.0001$, log-rank test) or BCG versus IKEPLUS ($P < 0.0001$, log-rank test). (**b**) Measurement of CFU from the lungs, spleens and livers of C57BL/6 mice in a separate experiment in which mice were immunized and challenged as described in **a**. Each symbol represents one mouse. # at base of the *y* axis for the liver CFU plot indicates that no colonies were obtained from IKEPLUS-vaccinated mice at day 202, consistent with clearance of Mtb infection in that tissue (entire organs were plated to give a limit of detection of 1 CFU). The CFU at day 100 was not significantly different between BCG- or IKEPLUS-immunized mice in any organ ($P > 0.05$, ANOVA). Data shown are pooled from two independent experiments. (**c**) Survival and lung CFU of C57BL/6 mice that were sham immunized (i.v. PBS; $n = 6$) or immunized by intravenous infection with IKE (5×10^7 CFU per mouse; $n = 6$) or IKEPLUS (5×10^7 CFU per mouse; $n = 6$) and subsequently challenged 6 weeks later with a high intravenous dose (5×10^7 CFU per mouse) of Mtb H37Rv. Differences in survival curves were significant for PBS versus IKEPLUS ($P = 0.0007$, log-rank test), PBS versus IKE ($P = 0.0049$, log-rank test) and IKEPLUS versus IKE ($P = 0.0246$, log-rank test). For lung CFU, asterisks indicate significant differences ($P < 0.05$, two-way ANOVA) compared to the PBS control group. Results shown are representative of four independent experiments.

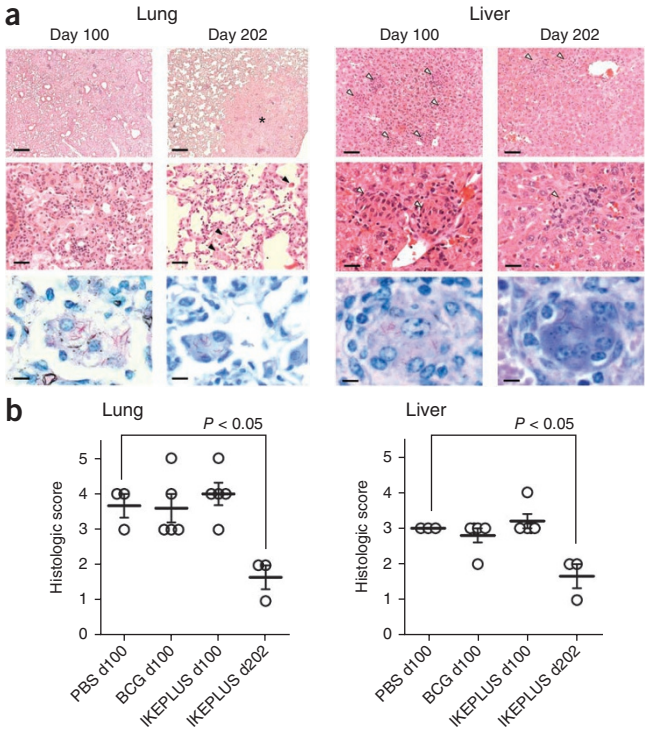

Figure 4 Improvement of histopathology in IKEPLUS-immunized mice during resolution of Mtb infection. (**a**) Representative images are shown for lungs (left) and livers (right) of C57BL/6 mice immunized with IKEPLUS and challenged with Mtb as described in **Figure 3**. Top and middle, H&E staining; bottom, AFB staining. Scale bars correspond to 650 nm, 40 nm and 10 nm in top, middle and bottom rows, respectively. The asterisk indicates an area of residual dense granulomatous infiltrate. Filled arrowheads indicate occasional macrophages in open alveoli in the lungs of mice with resolving inflammation at day 202. Open arrowheads mark granulomatous foci in the liver, which were also substantially resolved by day 202. AFBs were visualized in macrophages in lung and liver sections at both time points. (**b**) Quantitative scoring of histopathology confirming that all three groups showed similar pathology in the lungs and liver at day 100 ($P > 0.05$, two-way ANOVA). However, at day 202 the survivors from the IKEPLUS-immunized group showed significantly reduced pathology scores ($P < 0.05$ compared to all other groups at day 100; one-way ANOVA with Tukey post-test).

points after Mtb challenge (**Fig. 3b**). We observed this effect in lung, spleen and liver tissue at several time points after the challenge. Notably, the bacterial burdens of all tissues examined in IKEPLUS-immunized mice showed a continuing decline over time in mice that survived >100 d. By 200 d after Mtb challenge, these declines exceeded by >1,000-fold the maximum levels of CFU reduction achieved in those BCG-vaccinated mice that survived to day 100. Furthermore, CFU measurements were below the limit of detection in the livers of IKEPLUS-vaccinated and Mtb-challenged mice surviving >200 d, indicating a high level of bactericidal and potentially sterilizing immunity. In contrast to the long-term survival observed in a subset of IKEPLUS-immunized mice, no BCG-immunized mice survived more than 173 d after challenge, and BCG-immunized mice that survived to 100 d had a greater bacterial burden in all organs than did IKEPLUS-immunized mice (**Fig. 3b**). The Mtb genes present in IKEPLUS were necessary to induce highly protective immune responses, as mice sham-vaccinated with the parental IKE strain showed survival and bacterial burden after Mtb challenge that were only modestly better than those of naive mice (**Fig. 3c**).

Histopathological evaluation also revealed evidence of robust immunity in IKEPLUS-vaccinated mice. At 100 d after Mtb challenge, all mice showed moderate-to-severe diffuse granulomatous pneumonia, and at this time point there were no apparent differences in the lung histology (**Fig. 4a** and **Supplementary Fig. 6**) or severity of pneumonia on the basis of quantitative visual scoring (**Fig. 4b**) between mice immunized with saline, BCG or IKEPLUS. The severity of granulomatous inflammation in the spleens and livers from all treatment groups were likewise similar at day 100 after Mtb challenge (**Fig. 4b** and data not shown). However, lung tissues from IKEPLUS-immunized mice surviving >200 d after Mtb challenge showed clear evidence of gradually resolving granulomatous inflammation as compared to lung tissue at day 100, along with improvements in microscopic appearance (**Fig. 4a**) and significant reductions in the histological scores (**Fig. 4b**) in both lung and liver sections. Notably, we continued to observe low numbers of acid-fast bacilli (AFB) in small granuloma-like structures in the livers of IKEPLUS-immunized mice killed at more than 200 d after Mtb challenge (**Fig. 4a**), despite the lack of culturable bacilli in these tissues.

Efficacy of subcutaneously administered IKEPLUS as a vaccine

The unusually potent immune response elicited by intravenously administered IKEPLUS led us to assess its potential as a subcutaneously administered vaccine against tuberculosis in mice. As a first approach, we immunized mice subcutaneously with BCG or IKEPLUS and 8 weeks later challenged them with a high intravenous dose (1×10^8 CFU) of Mtb. Compared to BCG-immunized mice, mice immunized subcutaneously with IKEPLUS had significantly ($P < 0.01$) more serum IL-12 p40 upon challenge with Mtb (**Supplementary Fig. 7a**). Furthermore, mice immunized subcutaneously with IKEPLUS survived significantly longer after Mtb challenge than did BCG-immunized mice (**Fig. 5a**). Quantification of tissue bacterial burdens showed that subcutaneous immunization of mice with IKEPLUS led to an ~3-log reduction of CFU in the lung at 20 d after Mtb challenge compared to lung tissue in saline-immunized mice, which was nearly 2 logs better than the level of protection from BCG immunization (**Fig. 5a**).

To assess the vaccine efficacy of IKEPLUS in a more physiological setting, we immunized mice subcutaneously and then challenged them 1 month later by low-dose aerosol infection with Mtb (~100 CFU per mouse). Mice immunized subcutaneously with IKEPLUS showed a trend toward longer survival after Mtb challenge compared to BCG-immunized mice (**Fig. 5b**; mean survival 301 d versus 267 d; $P = 0.0898$, log-rank test). IKEPLUS vaccination resulted in significant reductions in CFU in lung and spleen tissues that were comparable to those achieved with BCG at 4 weeks (**Fig. 5b**). However, at 25 weeks after Mtb challenge, the reduction in CFU for IKEPLUS-immunized mice was maintained, whereas bacterial burdens in BCG-immunized mice increased to the level observed in sham-vaccinated mice (**Fig. 5b**).

Central role for CD4$^+$ T cells in immunity induced by IKEPLUS

The ability of IKEPLUS to enhance IL-12 p40 and IFN-γ production suggested enhanced T_H1 cell responses as a mechanism for heightened protective immunity in IKEPLUS-immunized mice. This idea was supported by cytokine profiles elicited in the immunization-challenge model (**Supplementary Fig. 7**), as mice immunized with either IKE or IKEPLUS showed rapid induction of IL-12 p40 and IFN-γ expression in the first 2 d after high-dose intravenous challenge with Mtb (**Supplementary Fig. 7b**). These data suggested

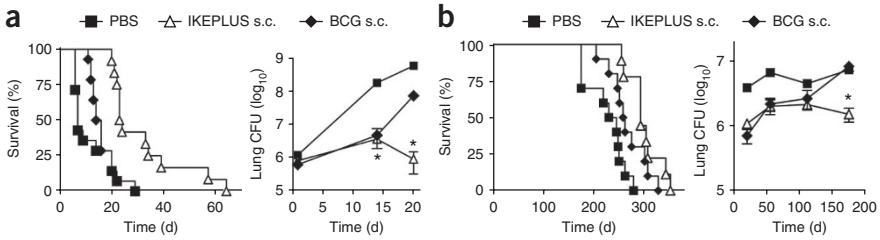

Figure 5 Protection from Mtb challenge by subcutaneous immunization with IKEPLUS. (**a**) Survival (left) of C57BL/6 mice ($n = 10$–14 per group) immunized subcutaneously with PBS, IKEPLUS (1×10^8 CFU per mouse), or BCG (1×10^6 CFU per mouse) and challenged 5 weeks later with a high intravenous dose (1×10^8 CFU per mouse) of Mtb H37Rv. CFU (right) data from the same experiment show means of three mice per group. The survival curve for IKEPLUS-immunized mice was significantly different from that of the BCG-immunized mice ($P < 0.001$, log-rank test). The CFU levels in lungs of IKEPLUS-immunized mice were significantly different from those of surviving saline-immunized mice at days 14 and 20 ($P < 0.01$, two-way ANOVA) and compared to BCG-immunized mice at day 20 ($P < 0.01$, two-way ANOVA). (**b**) Survival (left) of mice immunized subcutaneously with PBS ($n = 10$), 1×10^6 CFU of BCG ($n = 10$) or 1×10^8 CFU of IKEPLUS ($n = 9$) and challenged 1 month later with ~100 CFU of aerosolized Mtb H37Rv. The survival curves for IKEPLUS- and BCG-immunized mice were significantly different from that of PBS-immunized mice ($P < 0.05$, log-rank test). The survival curve for IKEPLUS was not significantly different from that of BCG-immunized mice ($P = 0.0898$, log-rank test). Lung CFU (right) from three mice per group from the same experiment showed that the IKEPLUS- and BCG-vaccinated groups had significantly reduced CFU compared to saline-immunized mice at days 21, 56 and 112 ($P < 0.05$, two-way ANOVA). IKEPLUS-immunized mice also showed lower CFU versus saline- or BCG-immunized mice at day 175 (*$P < 0.05$, two-way ANOVA). Results are representative of three independent experiments.

that the protective responses elicited by IKEPLUS immunization were associated with the induction of T_H1-type adaptive immunity. This hypothesis was further supported by our findings that *Rag1*$^{-/-}$ and IL-12 p40–deficient mice showed no significant change ($P > 0.25$) in their high susceptibility to Mtb challenge after immunization with IKEPLUS (**Supplementary Fig. 8a**).

As adaptive T cell immunity requires priming through peptide antigen presentation by major histocompatibility complex (MHC) class I

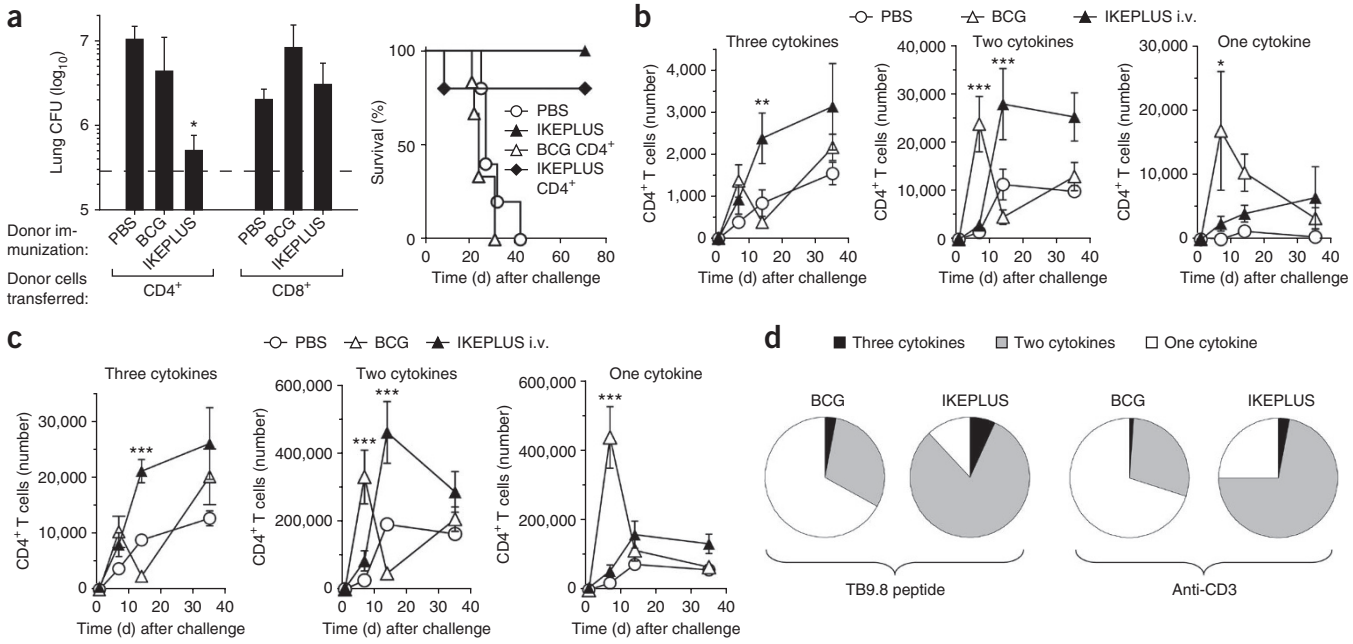

Figure 6 Role of CD4+ T cells in IKEPLUS-induced protective immunity. (**a**) Contributions of CD4+ and CD8+ subsets, as assessed by adoptive transfer of T cells from IKEPLUS-immunized mice. Naive recipient mice ($n = 5$ per group) were challenged 1 d after T cell transfer with *M. tuberculosis* (H37Rv, 1×10^7 CFU i.v. per mouse). Left, lung CFU of Mtb for mice killed 3 weeks after Mtb challenge. The dashed line indicates mean CFU in the lungs of five mice that were directly immunized with IKEPLUS (5×10^7 CFU per mouse i.v.) at 3 weeks before challenge. A negative control group of five sham-immunized mice that did not receive T cell transfer before challenge had CFU levels that were not significantly different from those of recipients of T cells from saline-immunized donors (not shown). *$P < 0.05$ compared to negative control group (ANOVA). This experiment was performed three times with similar results. Right, survival curves from similarly treated groups ($n = 5$) of mice from one experiment. IKEPLUS CD4+, adoptive transfer of CD4+ T cells from IKEPLUS-immunized donors; BCG CD4+, transfer of CD4+ T cells from BCG-immunized donors. Mice immunized intravenously with IKEPLUS directly or injected with PBS only were included as controls. The IKEPLUS CD4+ group was significantly different from the PBS group ($P = 0.035$, log-rank test) but not significantly different from the directly IKEPLUS-immunized group ($P = 0.3177$). (**b**) Cytokine production by CD4+ T cells in the lungs of mice immunized intravenously with PBS (sham) or IKEPLUS (5×10^7 CFU per mouse) or subcutaneously with BCG (1×10^6 CFU per mouse) and challenged 8 weeks later with Mtb H37Rv (1×10^7 CFU i.v.) ($n = 5$ mice per time point). The graphs indicate the absolute numbers of CD4+ T cells staining positively for three, two or one of the cytokines analyzed (IFN-γ, TNF and IL-2) after re-stimulation *in vitro* with a peptide representing the immunodominant epitope of TB9.8. Significant differences between the IKEPLUS- and BCG-vaccinated groups are indicated (*$P < 0.05$, **$P < 0.01$, ***$P < 0.001$, two-way ANOVA). Results shown are representative of two similar experiments. (**c**) Same as in **b** except that the cells were re-stimulated with plate-bound monoclonal antibodies to CD3 and CD28 before analysis. (**d**) Pie charts showing the relative fractions of CD4+ T cells at 14 d after Mtb challenge producing three, two or one of the cytokines with either specific antigen re-stimulation *in vitro* (TB9.8 peptide) or polyclonal activation (anti-CD3).

and MHC class II proteins, we analyzed the requirement for these molecules in the induction of protective immunity by IKEPLUS. We immunized MHC class I–deficient and MHC class II–deficient mice with IKEPLUS (intravenously), BCG (subcutaneously) or saline and then challenged them with a high intravenous dose (1×10^7 CFU per mouse) of virulent Mtb. Determination of bacterial loads showed that MHC class I–deficient mice immunized with IKEPLUS had significantly higher ($P < 0.05$) protection compared to saline-immunized MHC class I–deficient mice upon challenge with Mtb at both the 2-week and 4-week time points (**Supplementary Fig. 8b**). In contrast, the bacterial loads in IKEPLUS-immunized MHC class II–deficient mice killed at both 2 weeks and 4 weeks after challenge were not significantly different ($P > 0.05$) from those of saline-immunized MHC class II–deficient mice (**Supplementary Fig. 8b**). This suggests that the protective immunity elicited by IKEPLUS immunization is dependent on MHC class II presentation and therefore probably involves responses by $CD4^+$ T cells.

To further examine the involvement of $CD4^+$ T cells, we assessed the ability of purified T cell populations from IKEPLUS-immunized mice to transfer protection against Mtb challenge to naive mice. We immunized mice intravenously with IKEPLUS or saline or subcutaneously with BCG. After 3–6 weeks, we purified $CD4^+$ T cells from the spleens of immunized mice and then transferred them to naive mice. These mice were then challenged with a high intravenous dose (1×10^7 CFU per mouse) of Mtb. Lung CFU counts 3 weeks after challenge showed that significant protection was transferred by $CD4^+$ T cells from IKEPLUS-vaccinated donors, with a reduction in CFU nearly equivalent to that in mice that had been directly immunized with either intravenous IKEPLUS or subcutaneous BCG (**Fig. 6a**). Survival was also significantly extended in mice receiving $CD4^+$ T cells from IKEPLUS-immunized donors (**Fig. 6a**). As expected, $CD4^+$ T cells from sham-vaccinated mice did not transfer protection in this experiment, nor did $CD4^+$ T cells from BCG-vaccinated donors, consistent with earlier studies showing that transfer of BCG-induced immunity requires sublethal irradiation of recipients[36]. There was no transfer of protection using purified $CD8^+$ T cells from any of the donor groups. Thus, the $CD4^+$ T cell population from IKEPLUS-immunized mice seemed to contain the main pool of memory T cells responsible for activating protective immunity to challenge with Mtb.

We examined the multifunctionality of the $CD4^+$ T cell response in IKEPLUS-immunized mice by analyzing cytokine production by $CD4^+$ T cells infiltrating the lung at various time points after Mtb challenge (**Fig. 6b–d** and **Supplementary Fig. 9**). Upon re-stimulation *in vitro* with a peptide corresponding to an MHC class II ($I\text{-}A^b$)-presented epitope of the TB9.8 (esxG) protein (**Supplementary Fig. 1**), we observed a substantially different pattern of cytokine production between BCG- and IKEPLUS-immunized mice (**Fig. 6b**). Using simultaneous analysis of three cytokines (IFN-γ, tumor necrosis factor (TNF) and IL-2), we observed an increase of $CD4^+$ T cells producing two or three of these cytokines in IKEPLUS-immunized compared with BCG-immunized mice (**Fig. 6b**,**d**) in response to stimulation by TB9.8. This was particularly evident at 2 or more weeks after Mtb challenge. In marked contrast, $CD4^+$ T cells producing two or three of these cytokines accumulated more gradually in the IKEPLUS-immunized mice, but their levels were sustained to the latest time points examined (that is, day 36). We observed a similar pattern in total lung-derived $CD4^+$ T cells after re-stimulation *in vitro* with CD3-specific antibody (**Fig. 6c**,**d**).

DISCUSSION

In the current study we have demonstrated a major role for the *esx-3* locus of Msmeg in modifying the mammalian host immune response, and in so doing we have generated a new and highly effective candidate vaccine for tuberculosis. Although Msmeg is a saprophytic organism rarely reported as a cause of clinical infections[37,38], our high-dose intravenous inoculation protocol in mice revealed its ability to establish a rapidly fatal experimental infection. This cryptic virulence of Msmeg was dependent on an intact ESX-3 secretion system, as deletion of the *esx-3* genes generated a strain (IKE) that was rapidly cleared without sequellae. We observed clearance of IKE in mice lacking various components of innate and adaptive immunity, but not in MyD88-deficient mice. Overall, these findings are consistent with a role for ESX-3 in mediating resistance to MyD88-dependent bactericidal effects in mice. As mice defective in Toll-like receptor 2 and IL-1R signaling retained resistance to high-dose infection with IKE (**Supplementary Table 1**), these MyD88-dependent receptors are probably not involved.

How the *esx-3* locus contributes to resistance to MyD88-dependent killing of mycobacteria remains to be determined. It is possible that this effect is related to the iron-acquisition function of ESX-3, although many other possibilities can be envisioned. For example, ESX-3–secreted substrates may directly interact with innate immune signaling or effector molecules and modulate the response to intracellular infection. So far, only one secreted substrate, EsxH (TB10.4) has been directly documented for this system[34]. However, the Cfp-10 paralog EsxG (TB9.8) is also likely to be secreted by ESX-3, and annotation of the *esx-3* locus reveals genes for proteins belonging to the PE and PPE families, other members of which are known to be exported by the ESX-5 system and to modulate macrophage responses[39]. As in the case of ESX-1, the secreted substrates of ESX-3 may potentially be encoded by genes mapping to chromosomal sites outside the locus encoding the secretion system[40].

Inoculation with IKE induced a more robust T_H1-priming cytokine milieu and a more rapid and vigorous IFN-γ response as compared to inoculation with the parental Msmeg strain. Preliminary analysis also suggested that IKE stimulated increased phagosome maturation during macrophage infection (K.A.S. and W.R.J. Jr., unpublished data), which could lead to increased processing and presentation of bacterial antigens. When we added Mtb antigens from a cosmid encoding genes *Rv0278–Rv0303* to IKE, we derived a strain (IKEPLUS) that elicited a high level of protective immunity when used as a live attenuated vaccine against Mtb in mice. These findings contrast with many earlier studies examining Msmeg as a vaccine vector delivered either intranasally or subcutaneously, which showed no significant improvement in efficacy compared to BCG[41–43]. We hypothesize that the superior vaccine potency of IKEPLUS is attributable to the loss of innate immune evasion mediated by *esx-3*. The modified innate immune response to Msmeg lacking *esx-3* generates a cytokine milieu that favors the priming of T_H1 cell responses, as indicated by the enhanced systemic IL-12 and IFN-γ levels observed. This, in turn, leads to an improved adaptive immunity, which may be directed against the Mtb antigens encoded by IKEPLUS.

Notably, the robust adaptive immune response induced by IKEPLUS was potent and long-lived, as indicated by the marked decline in Mtb bacilli in the tissues of IKEPLUS-immunized animals. To our knowledge, neither BCG nor any of the attenuated Mtb vaccine strains described to date induces such obvious or prolonged bactericidal immunity. Several reports have described modified-BCG or other novel tuberculosis vaccine regimens that deliver modestly better protective immunity against Mtb than does standard BCG (for example, up to a 1-log improvement in reduction in CFU counts in the lungs)[6,44–49]. However, none of these 'improved' tuberculosis

vaccines has been shown to produce the sustained decline or magnitude of reduction (>3 logs) in Mtb tissue burdens that we observed in IKEPLUS-immunized mice.

Most notably, our observation of apparent sterility in the livers of IKEPLUS-immunized animals surviving past 200 d after Mtb challenge may represent the first documented example of the elimination of this organism from a tissue by immunological mechanisms alone. These findings reveal a capacity of the mammalian adaptive immune system to orchestrate potent bactericidal sterilization in Mtb-infected tissues. This result was most apparent when we administered IKEPLUS intravenously, which is not a feasible route for standard vaccination, and even with intravenous inoculation only a small fraction (10–20%) of IKEPLUS-immunized mice achieved long-term survival after Mtb challenge. Thus, further improvements will be needed to optimize the efficacy of IKEPLUS vaccination for translational development and implementation as a vaccine in humans. This may involve combining IKEPLUS immunization with other types of immunogens in prime-boost regimens. Nevertheless, the substantial bactericidal immunity we observed after subcutaneous immunization with IKEPLUS in both the intravenous and aerosol Mtb challenge models is encouraging. Although the magnitude of this immunity was not as great as that observed after intravenous immunization, it was still substantially greater and longer lasting than the protection induced by standard BCG vaccination. We are currently in the process of determining which genes of the integrated cosmid in IKEPLUS are required for induction of protective immunity and are carrying out further modifications with the intent of increasing the vaccine potency of IKEPLUS when administered by clinically acceptable routes.

Determining of the mechanism of bacterial killing in IKEPLUS-immunized mice is clearly a crucial next step. Our finding that transfer of $CD4^+$ T cells from IKEPLUS-immunized mice into naive mice was sufficient to confer substantial protection strongly suggested that this mechanism involved generation of a unique memory $CD4^+$ T cell population. To the best of our knowledge, this is the first example in an Mtb infection model of adoptively transferred immunity from immunized mice to naive mice without previous irradiation for lymphocyte depletion of the recipient mice[36]. This further suggests that the response stimulated by IKEPLUS is qualitatively different from that induced by BCG, or unusually potent. A qualitative effect on the $CD4^+$ T cell response was also indicated by increased multifunctionality of the cytokine-producing cells responding to the TB9.8 antigen in the lungs of IKEPLUS-immunized mice after Mtb challenge. Notably, we also observed this pattern for $CD4^+$ T cells from IKEPLUS-vaccinated mice stimulated *ex vivo* by monoclonal anti-CD3 antibody, suggesting that this multifunctional program had been imprinted on the great majority of $CD4^+$ T cells accumulating after Mtb challenge in the lungs of IKEPLUS-immunized but not BCG-immunized mice.

Although $CD4^+$ T cells seem to be the crucial memory cells involved in initiating the bactericidal response, it is likely that these cells recruit additional effectors that may ultimately be partially or entirely responsible for the actual killing of the mycobacteria. Such downstream effectors could include various myeloid subsets and innate-like lymphocytes with potent effector functions such as natural killer cells, NKT cells or γδ T cells[50]. B lymphocytes and secreted antibodies may also have a role, as preliminary experiments using western blotting to assess antimycobacterial antibody responses in the sera of immunized and challenged mice showed marked differences between IKEPLUS- and BCG-immunized mice (K.A.S. and W.R.J. Jr., unpublished data). Determining the interplay between these various immune effector mechanisms in bringing about clearance of newly introduced or established Mtb infections will be a major focus of further studies on the use of IKEPLUS as a candidate tuberculosis vaccine.

METHODS

Methods and any associated references are available in the online version of the paper at http://www.nature.com/naturemedicine/.

Note: Supplementary information is available on the Nature Medicine website.

ACKNOWLEDGMENTS

We acknowledge the support of US National Institutes of Health (NIH) grants AI063537, AI093649, AI092448, AI26170 and AI051519 (Einstein Center for AIDS Research), and the Bill and Melinda Gates Foundation Collaboration for AIDS Vaccine Discovery. K.A.S. acknowledges support from the Albert Einstein College of Medicine's Institutional AIDS Training Grant T32-AI007501. We thank C. Harding, L. Ramachandra, G. Lauvau and S. Morris for advice and suggestions, as well as C. Colon-Berezin and S. Tiwari for helpful editing of the manuscript. Flow cytometry studies were carried out using core facilities supported by the Einstein Cancer Center (NIH/National Cancer Institute CA013330) and the Einstein Center for AIDS Research (NIH AI051519).

AUTHOR CONTRIBUTIONS

K.A.S. constructed bacterial strains, performed or contributed to the design of most experiments, and analyzed and interpreted data. D.N.D. carried out portions of the infection and challenge experiments. M.F.G. contributed to the T cell adoptive transfer studies and designed, performed and analyzed all flow cytometry analyses. T.H. participated in design and construction of bacterial strains and in the performance of mouse infection and challenge experiments. P.J. contributed to construction of bacterial strains. M.M.V. and M.H.-T. assisted with experiments analyzing responding T cell populations. R.S.S. analyzed and scored the histopathology samples. B.C., M.C., J.K. and R.L. carried out mouse infections, organ harvesting and quantification of bacilli in tissues. D.O., J.C., I.M.O., S.A.P. and W.R.J. Jr. designed and interpreted experiments. K.A.S., S.A.P. and W.R.J. Jr. wrote the manuscript.

COMPETING FINANCIAL INTERESTS

The authors declare no competing financial interests.

Published online at http://www.nature.com/naturemedicine/.
Reprints and permissions information is available online at http://www.nature.com/reprints/index.html.

1. Dye, C., Scheele, S., Dolin, P., Pathania, V. & Raviglione, M.C. Consensus statement. Global burden of tuberculosis: estimated incidence, prevalence, and mortality by country. WHO Global Surveillance and Monitoring Project. *J. Am. Med. Assoc.* **282**, 677–686 (1999).
2. Gandhi, N.R. *et al.* Extensively drug-resistant tuberculosis as a cause of death in patients co-infected with tuberculosis and HIV in a rural area of South Africa. *Lancet* **368**, 1575–1580 (2006).
3. Colditz, G.A. *et al.* Efficacy of BCG vaccine in the prevention of tuberculosis. Meta-analysis of the published literature. *J. Am. Med. Assoc.* **271**, 698–702 (1994).
4. Corbett, E.L. *et al.* The growing burden of tuberculosis: global trends and interactions with the HIV epidemic. *Arch. Intern. Med.* **163**, 1009–1021 (2003).
5. Hesseling, A.C. *et al.* The risk of disseminated bacille Calmette-Guerin (BCG) disease in HIV-infected children. *Vaccine* **25**, 14–18 (2007).
6. Hinchey, J. *et al.* Enhanced priming of adaptive immunity by a proapoptotic mutant of *Mycobacterium tuberculosis*. *J. Clin. Invest.* **117**, 2279–2288 (2007).
7. Orme, I.M. Preclinical testing of new vaccines for tuberculosis: a comprehensive review. *Vaccine* **24**, 2–19 (2006).
8. Skeiky, Y.A. & Sadoff, J.C. Advances in tuberculosis vaccine strategies. *Nat. Rev. Microbiol.* **4**, 469–476 (2006).
9. Sander, C.R. *et al.* Safety and immunogenicity of a new TB vaccine, MVA85A, in *M. tuberculosis* infected individuals. *Am. J. Respir. Crit. Care Med.* **179**, 724–733 (2009).
10. Armstrong, J.A. & Hart, P.D. Response of cultured macrophages to *Mycobacterium tuberculosis*, with observations on fusion of lysosomes with phagosomes. *J. Exp. Med.* **134**, 713–740 (1971).
11. Fulton, S.A. *et al.* Inhibition of major histocompatibility complex II expression and antigen processing in murine alveolar macrophages by *Mycobacterium bovis* BCG and the 19-kilodalton mycobacterial lipoprotein. *Infect. Immun.* **72**, 2101–2110 (2004).
12. Pai, R.K. *et al.* Prolonged toll-like receptor signaling by *Mycobacterium tuberculosis* and its 19-kilodalton lipoprotein inhibits gamma interferon-induced regulation of selected genes in macrophages. *Infect. Immun.* **72**, 6603–6614 (2004).

13. Dao, D.N. *et al.* Mycolic acid modification by the mmaA4 gene of *M. tuberculosis* modulates IL-12 production. *PLoS Pathog.* **4**, e1000081 (2008).
14. Baena, A. & Porcelli, S.A. Evasion and subversion of antigen presentation by *Mycobacterium tuberculosis*. *Tissue Antigens* **74**, 189–204 (2009).
15. Mahairas, G.G., Sabo, P.J., Hickey, M.J., Singh, D.C. & Stover, C.K. Molecular analysis of genetic differences between *Mycobacterium bovis* BCG and virulent *M. bovis*. *J. Bacteriol.* **178**, 1274–1282 (1996).
16. Behr, M.A. *et al.* Comparative genomics of BCG vaccines by whole-genome DNA microarray. *Science* **284**, 1520–1523 (1999).
17. Lewis, K.N. *et al.* Deletion of RD1 from *Mycobacterium tuberculosis* mimics bacille Calmette-Guerin attenuation. *J. Infect. Dis.* **187**, 117–123 (2003).
18. Pym, A.S. *et al.* Recombinant BCG exporting ESAT-6 confers enhanced protection against tuberculosis. *Nat. Med.* **9**, 533–539 (2003).
19. Stanley, S.A., Raghavan, S., Hwang, W.W. & Cox, J.S. Acute infection and macrophage subversion by *Mycobacterium tuberculosis* require a specialized secretion system. *Proc. Natl. Acad. Sci. USA* **100**, 13001–13006 (2003).
20. Hsu, T. *et al.* The primary mechanism of attenuation of bacillus Calmette-Guerin is a loss of secreted lytic function required for invasion of lung interstitial tissue. *Proc. Natl. Acad. Sci. USA* **100**, 12420–12425 (2003).
21. MacGurn, J.A. & Cox, J.S. A genetic screen for *Mycobacterium tuberculosis* mutants defective for phagosome maturation arrest identifies components of the ESX-1 secretion system. *Infect. Immun.* **75**, 2668–2678 (2007).
22. de Jonge, M.I. *et al.* ESAT-6 from *Mycobacterium tuberculosis* dissociates from its putative chaperone CFP-10 under acidic conditions and exhibits membrane-lysing activity. *J. Bacteriol.* **189**, 6028–6034 (2007).
23. Xu, J. *et al.* A unique Mycobacterium ESX-1 protein co-secretes with CFP-10/ESAT-6 and is necessary for inhibiting phagosome maturation. *Mol. Microbiol.* **66**, 787–800 (2007).
24. Smith, J. *et al.* Evidence for pore formation in host cell membranes by ESX-1-secreted ESAT-6 and its role in *Mycobacterium marinum* escape from the vacuole. *Infect. Immun.* **76**, 5478–5487 (2008).
25. van der Wel, N. *et al.* M. tuberculosis and M. leprae translocate from the phagolysosome to the cytosol in myeloid cells. *Cell* **129**, 1287–1298 (2007).
26. Gey Van Pittius, N.C. *et al.* The ESAT-6 gene cluster of *Mycobacterium tuberculosis* and other high G+C Gram-positive bacteria. *Genome Biol.* **2**, research0044 (2001).
27. Stinear, T.P. *et al.* Insights from the complete genome sequence of *Mycobacterium marinum* on the evolution of *Mycobacterium tuberculosis*. *Genome Res.* **18**, 729–741 (2008).
28. Maciag, A. *et al.* Global analysis of the *Mycobacterium tuberculosis* Zur (FurB) regulon. *J. Bacteriol.* **189**, 730–740 (2007).
29. Rodriguez, G.M., Voskuil, M.I., Gold, B., Schoolnik, G.K. & Smith, I. ideR, an essential gene in *Mycobacterium tuberculosis:* role of IdeR in iron-dependent gene expression, iron metabolism, and oxidative stress response. *Infect. Immun.* **70**, 3371–3381 (2002).
30. Talaat, A.M., Lyons, R., Howard, S.T. & Johnston, S.A. The temporal expression profile of *Mycobacterium tuberculosis* infection in mice. *Proc. Natl. Acad. Sci. USA* **101**, 4602–4607 (2004).
31. Dubnau, E., Chan, J., Mohan, V.P. & Smith, I. Responses of *Mycobacterium tuberculosis* to growth in the mouse lung. *Infect. Immun.* **73**, 3754–3757 (2005).
32. Sassetti, C.M., Boyd, D.H. & Rubin, E.J. Genes required for mycobacterial growth defined by high density mutagenesis. *Mol. Microbiol.* **48**, 77–84 (2003).
33. Sassetti, C.M. & Rubin, E.J. Genetic requirements for mycobacterial survival during infection. *Proc. Natl. Acad. Sci. USA* **100**, 12989–12994 (2003).
34. Siegrist, M.S. *et al.* Mycobacterial ESX-3 is required for mycobactin-mediated iron acquisition. *Proc. Natl. Acad. Sci. USA* **106**, 18792–18797 (2009).
35. Flynn, J.L. & Chan, J. Immunology of tuberculosis. *Annu. Rev. Immunol.* **19**, 93–129 (2001).
36. Orme, I.M. & Collins, F.M. Protection against *Mycobacterium tuberculosis* infection by adoptive immunotherapy. Requirement for T cell-deficient recipients. *J. Exp. Med.* **158**, 74–83 (1983).
37. Pierre-Audigier, C. *et al.* Fatal disseminated *Mycobacterium smegmatis* infection in a child with inherited interferon gamma receptor deficiency. *Clin. Infect. Dis.* **24**, 982–984 (1997).
38. Kumar, K.J., Chandra, J., Mandal, R.N., Dutta, R. & Jain, N.K. Fatal pulmonary infection caused by *Mycobacterium smegmatis* in an infant. *Indian J. Pediatr.* **62**, 619–621 (1995).
39. Abdallah, A.M. *et al.* The ESX-5 secretion system of *Mycobacterium marinum* modulates the macrophage response. *J. Immunol.* **181**, 7166–7175 (2008).
40. Raghavan, S., Manzanillo, P., Chan, K., Dovey, C. & Cox, J.S. Secreted transcription factor controls *Mycobacterium tuberculosis* virulence. *Nature* **454**, 717–721 (2008).
41. Yang, C. *et al.* GLS/IL-12-modified *Mycobacterium smegmatis* as a novel anti-tuberculosis immunotherapeutic vaccine. *Int. J. Tuberc. Lung Dis.* **13**, 1360–1366 (2009).
42. Yi, Z. *et al.* Recombinant *M. smegmatis* vaccine targeted delivering IL-12/GLS into macrophages can induce specific cellular immunity against *M. tuberculosis* in BALB/c mice. *Vaccine* **25**, 638–648 (2007).
43. Yeremeev, V.V. *et al.* The 19-kD antigen and protective immunity in a murine model of tuberculosis. *Clin. Exp. Immunol.* **120**, 274–279 (2000).
44. Sun, R. *et al.* Novel recombinant BCG expressing perfringolysin O and the over-expression of key immunodominant antigens; pre-clinical characterization, safety and protection against challenge with *Mycobacterium tuberculosis*. *Vaccine* **27**, 4412–4423 (2009).
45. Kita, Y. *et al.* Novel recombinant BCG and DNA-vaccination against tuberculosis in a cynomolgus monkey model. *Vaccine* **23**, 2132–2135 (2005).
46. van Dissel, J.T. *et al.* Ag85B-ESAT-6 adjuvanted with IC31 promotes strong and long-lived *Mycobacterium tuberculosis* specific T cell responses in naive human volunteers. *Vaccine* **28**, 3571–3581 (2010).
47. Williams, A. *et al.* Boosting with poxviruses enhances *Mycobacterium bovis* BCG efficacy against tuberculosis in guinea pigs. *Infect. Immun.* **73**, 3814–3816 (2005).
48. Whelan, K.T. *et al.* Safety and immunogenicity of boosting BCG vaccinated subjects with BCG: comparison with boosting with a new TB vaccine, MVA85A. *PLoS ONE* **4**, e5934 (2009).
49. Vordermeier, H.M. *et al.* Viral booster vaccines improve *Mycobacterium bovis* BCG-induced protection against bovine tuberculosis. *Infect. Immun.* **77**, 3364–3373 (2009).
50. Bendelac, A., Bonneville, M. & Kearney, J.F. Autoreactivity by design: innate B and T lymphocytes. *Nat. Rev. Immunol.* **1**, 177–186 (2001).

ONLINE METHODS

Mycobacterial infections and Mtb challenge studies. Mycobacterial strains and mutant construction are described in the **Supplementary Methods**. *M. smegmatis* cultures for infection were grown from low-passage freezer stocks to mid-log phase, subcultured and grown to an A_{600} of 0.1–0.5, washed and resuspended in PBS plus 0.05% Tween-80 (PBS/T). Bacteria were sonicated before infection to obtain single-cell suspensions. Mice were infected with Msmeg strains either through the tail vein (5×10^7 CFU in 200 µl), or subcutaneously (1×10^7 CFU in 100 µl) at the scruff of the neck. BCG cultures were grown to mid-log phase, washed, resuspended in PBS/T and sonicated before infection. Mice were vaccinated with BCG subcutaneously at the scruff of the neck with 1×10^6 CFU in 100 µl. Msmeg was heat killed by warming to 80 °C for 30 min, or ultraviolet light–irradiated by exposure for 30 min to a 65-Watt ultraviolet lamp at a distance of 6 inches.

For aerosol or intravenous challenge with Mtb, a low-density freezer stock of H37Rv was grown in 7H9 liquid medium to an A_{600} of 0.4–0.8. For intravenous infections, bacterial stocks were diluted to give a dose of 1×10^7 CFU or 1×10^8 CFU in 200 µl PBS/T injected per mouse via the tail vein. For aerosol infections, 2×10^6 CFU ml^{-1} of bacteria in PBS/T plus 0.04% (vol/vol) Antifoam Y-30 (Sigma) was placed in a nebulizer attached to an airborne infection system (University of Wisconsin Mechanical Engineering Workshop). Mice were exposed to aerosol for 40 min, during which approximately 100 bacteria were deposited in the lungs of each animal. Tissue bacterial loads in tissues for both intravenous and aerosol infections were determined by plating organ homogenates onto 7H10 agar OADC plates. Colonies were counted after 21 d of incubation at 37 °C.

Serum cytokine analysis. Infected mice were bled at the time of killing or by an orbital survival bleed. Serum was collected in Sarstedt Z-gel 1.5 microcentrifuge tubes with a clotting activator in the bottom according to the manufacturer's instructions, and filtered through a 0.22-µm SpinX column (Costar) to remove any bacteria. Cytokine was measured by either sandwich ELISA with the Biosource International kit (Camarillo) or by an MS2400 Mouse T_H1/T_H2-9 Ultra Sensitive plate and reagent kit (Meso Scale Discovery) for multiplex detection of nine cytokines.

Flow cytometry for cell-surface markers and intracellular cytokines. For analysis of cytokine-producing CD4$^+$ T cells, lung cell suspensions were isolated (**Supplementary Methods**) and placed in 96-well plates in RPMI-1640 with 10% (vol/vol) FCS. The samples were re-stimulated with 10 µg ml^{-1} TB9.8 peptide or plate-bound monoclonal antibody to mouse CD3ε (clone 145-2C11), with unstimulated wells serving as negative controls. The TB9.8 peptide used (TB9.8$_{43–58}$; ESSAAFQAAHARFVAA) represents an immunodominant epitope identified in BCG-vaccinated mice (M.F.G. and S.A.P., unpublished data). Samples were combined with 1 µg ml^{-1} soluble antibody to mouse CD28 (clone 37.51). After 2 h at 37 °C, 10 µg ml^{-1} of Brefeldin-A (Sigma) was added to all samples, followed by incubation for 4 h. Cells were stained with Blue LIVE/DEAD viability dye (Invitrogen) followed by antibody to FcγRII/III (clone 2.4G2; American Type Culture Collection), with fluorochrome-conjugated monoclonal antibodies for surface staining: antibody to CD3ε (clone 145-2C11; eBioscience), antibody to CD44 (clone IM7; eBioscience), antibody to CD8α (clone 53-6.7; BD Bioscience) and antibody to CD4 (clone GK1.5; BD Bioscience). Cells were fixed with 2% (vol/vol) paraformaldehyde, washed with permeabilization buffer (PBS with 1 mM Ca^{2+}, 1 mM Mg^{2+}, 1 mM HEPES, 2% (vol/vol) FCS and 0.1% (wt/vol) saponin) and then blocked in permeabilization buffer plus 5% (vol/vol) normal mouse serum (Jackson ImmunoResearch Laboratories). Intracellular cytokines were detected with fluorochrome-conjugated antibodies to IL-2 (clone JES6-5H4; eBioscience), IFN-γ (clone XMG1.2) and TNF-α (MP6-XT22) (both from BD Biosciences). Data were acquired on an LSR II flow cytometer (BD Biosciences), and data analysis was performed using FlowJo software (Tree Star).

T cell adoptive transfer. Donor mice were immunized intravenously with PBS or IKEPLUS (5×10^7 CFU per mouse) or subcutaneously with BCG (1×10^6 CFU per mouse). After 4 weeks, spleens were mechanically disrupted, and single-cell suspensions were prepared in PBS with 0.5% (wt/vol) BSA by passage through a 70-µm filter. CD4$^+$ and CD8$^+$ T cells were purified with a mouse CD4$^+$ and CD8$^+$ T cell isolation kit (Miltenyi Biotech), using cocktails of biotinylated monoclonal antibodies for negative selection of the desired cell population (antibodies to CD11b, CD11c, CD19, CD45R (B220), CD49b (DX5), CD105, antibody to MHC class II and Ter-119 along with antibody to CD8α for CD4$^+$ T cell isolation, and the same cocktail except with antibody to CD4 replacing antibody to CD8α for CD8$^+$ T cell isolation). After labeling with the biotin-conjugated antibody cocktails, MACS microbeads conjugated with anti-biotin reagent were added, and the untouched CD4$^+$ or CD8$^+$ T cells were isolated by passing the suspension through an AutoMACS PRO separator. Purity of isolated populations was 92–96%. Adoptive transfer was done by injection of 3×10^6 purified CD4$^+$ or CD8$^+$ T cells via the lateral tail vein.

Additional methods. Detailed methodology is described in the **Supplementary Methods**.